Crystal Structure of Human Cyclin-Dependent Kinase 2 in Complex with the Adenine-Derived Inhibitor H717

Matthias K. Dreyer,*,† David R. Borcherding,‡ Jennifer A. Dumont,‡,|| Norton P. Peet,‡ Joseph T. Tsay,‡ Paul S. Wright,‡ Alan J. Bitonti,‡,|| Jian Shen,‡ and Sung-Hou Kim*,†

Department of Chemistry and Lawrence Berkeley National Laboratory, University of California, Berkeley, California 94720, and Aventis Pharmaceuticals, Inc., Route 202-206, Bridgewater, New Jersey 08807

Received July 27, 2000

Cyclin-dependent kinases (CDKs) are regulatory proteins of the eukaryotic cell cycle. They act after association with different cyclins, the concentrations of which vary throughout the progression of the cell cycle. As central mediators of cell growth, CDKs are potential targets for inhibitory molecules that would allow disruption of the cell cycle in order to evoke an antiproliferative effect and may therefore be useful as cancer therapeutics. We synthesized several inhibitory 2,6,9-trisubstituted purine derivatives and solved the crystal structure of one of these compounds, H717, in complex with human CDK2 at 2.6 Å resolution. The orientation of the C^2-*p*-diaminocyclohexyl portion of the inhibitor is strikingly different from those of similar moieties in other related inhibitor complexes. The N^9-cyclopentyl ring fully occupies a space in the enzyme which is otherwise empty, while the C^6-*N*-aminobenzyl substituent points out of the ATP-binding site. The structure provides a basis for the further development of more potent inhibitory drugs.

Introduction

The progression of the eukaryotic cell cycle is tightly controlled by cyclin-dependent kinases (CDKs). The activity of this well-conserved family of serine/threonine protein kinases is regulated through multiple mechanisms such as transcriptional and translational control, phosphorylation, complex formation between catalytic and regulatory (cyclin) subunits, degradation of cyclins, and interaction with CDK inhibitory proteins (CKIs), e.g. p16, p21, and p27.[1] While monomeric CDKs are virtually inactive, complex formation with various cyclins provides a basal kinase activity which can subsequently be enhanced through phosphorylation of a threonine residue (Thr160 in human CDK2, Thr161 in cdc2) by a CDK activating kinase.[2,3]

In animal cells CDK2 is believed to play a major role in the onset of DNA replication. In the late G1 phase of the cell cycle, CDK2 is activated when it complexes with cyclin E and subsequently triggers the passage into the synthetic (S) phase. During S phase, the concentration of cyclin E decreases and CDK2 exchanges its regulatory subunit for cyclin A, which is active until G2 phase, when other CDKs are activated.[4] Currently, 9 different human CDKs (CDK1−9) and 10 cyclins (cyclin A−K) have been described. Several cellular targets of CDK2 have been identified, among them the tumor suppressor pRb,[5] the transcription factor E2F-1,[6] and the oncoprotein b-myb.[7] Recently, several crystal structures have been determined (the CDK2:ATP:Mg^{2+} complex,[8] the CDK2:cyclin A complex,[9] and the tertiary complex CDK2:cyclin A:p16[10]), which have greatly contributed to the understanding of CDK regulation and function.

Like several other protein kinases, CDK2 consists of a relatively small N-terminal domain that is rich in *β*-sheet structure and a larger C-terminal domain which is predominantly α-helical. The ATP-binding site is located in a pocket between the two domains. Upon association with cyclin A, CDK2 undergoes large conformational changes and activates the kinase activity through a rearrangement of active site residues.[9]

Malfunctioning of the cell cycle control mechanism may lead to enhanced CDK activity and uncontrolled cell proliferation. Indeed, several cancer types have been associated with mutations in CKI genes[11,12] and other regulators. Therefore, CDKs have become a target for the development of inhibitors which could function as antitumor agents.[13−17]

Numerous chemical compounds have been reported which inhibit cell cycle progression by binding to CDKs and thus possess great therapeutic potential.[15,18] Among these substances, ATP analogous 2,6,9-trisubstituted adenines such as olomoucine, roscovitine, and purvalanol[13] and their derivatives have been shown to be relatively specific for certain CDKs and have IC_{50} values in the micromolar to nanomolar range. As was shown by the crystal structures of CDK2:inhibitor complexes,[13,19,20] the inhibitors bind to and block the ATP pocket in the active site, but the binding mode of the adenine ring is quite different from that of the adenine portion of ATP.

In our study we report the crystal structure of the complex between human CDK2 and H717, a new olomoucine-derived highly potent CDK2 inhibitor.

* To whom correspondence should be addressed. For M.K.D.: Current address: Physiologische Chemie II, Biozentrum der Universität Würzburg, Am Hubland, 97074 Würzburg, Germany. E-mail: dreyer@biozentrum.uni-wuerzburg.de. For S.-H.K.: Phone: (+1)-510-486-4333. Fax: (+1)-510-486-5272. E-mail: shkim@lbl.gov.

† University of California.

‡ Aventis Pharmaceuticals, Inc.

|| Current address: Syntonix Pharmaceuticals, Inc., 9 Fourth Ave., Waltham, MA 02451.

10.1021/jm001043t CCC: $20.00
Published on Web 12/21/2000

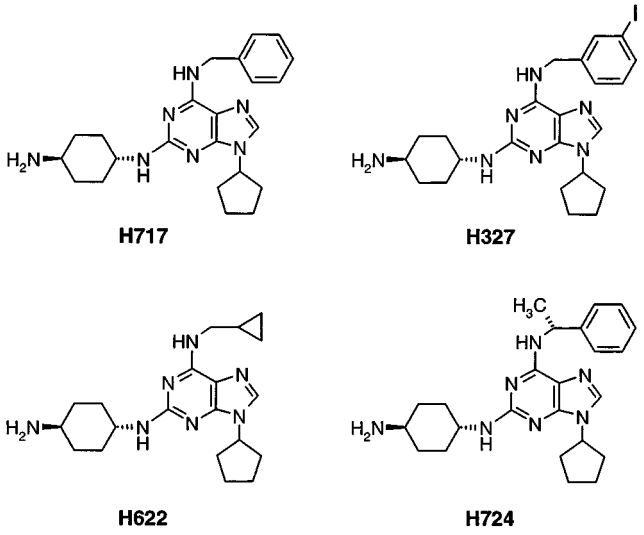

Figure 1. Structures of the 2,6,9-trisubstituted adenine derivatives investigated in this study.

Table 1. Inhibition of CDKs[a]

compd	IC$_{50}$, nM		
	CDK2	CDK4	CDK1
H327	50	2000	226
H622	24	780	70
H717	48	3600	52
H724	720	8800	2000

[a] Enzyme activities were measured as described in the Experimental Section in the presence of increasing drug concentrations. The IC$_{50}$ values represent the 50% inhibitory concentration.

Results

Inhibition of CDK2 by H717. 2,6,9-Trisubstituted purines are ATP analogues that are known to inhibit CDK2 activity by binding to the active site of the enzyme. We have synthesized a series of 6-substituted 2-[*trans*-(4-aminocyclohexyl)amino]-9-cyclopentylpurine derivatives (Figure 1) and tested them for inhibition of CDK2:cyclin E activity in assays using retinoblastoma protein as a substrate (Table 1). Three of the four substances showed IC$_{50}$ values between 24 and 50 nM and were thus by a factor of ca. 25-fold more effective than roscovitine (0.65 μM[19]) and only slightly less effective than purvalanol B (9 nM[13]). One of our compounds, H724, has an IC$_{50}$ value of 720 nM. This 10-fold decrease in inhibitory power is caused by an additional methyl group at C-19 in the benzylamino substituent, which is not present in any of the other compounds. Compounds H622, H327, and H717 inhibited the growth of human tumor cells in vitro with mean IC$_{50}$ values of 1.2−2.2 μM in comparison to H724 which had a mean IC$_{50}$ value of 5.6 μM for eight different cell lines (Table 2).

To reveal the chemical basis for the binding behavior, we solved the crystal structure of the complex between human CDK2 and H717.

Overall Protein Structure. The final protein model comprises residues 1−36, 46−148, and 163−298. The typically mobile regions 37−45 and 149−162 (the so-called T-loop) of the enzyme exhibited only poor electron density and could not be traced. Thirty water molecules were fitted into the model. The free *R*-factor of the final model is 24.2% (R_{conv} = 20.1%; further crystallographic data are listed in Table 3). All residues except for Asn74, which is located in a highly mobile loop, lie within allowed regions of the Ramachandran plot.

Table 2. Effect of Compounds on Human Tumor Cell Growth in Vitro[a]

tumor type	cell line	proliferation: IC$_{50}$, μM			
		H622	H327	H717	H724
breast	MCF-7	1.3	0.6	1.4	3.3
	MDA-MB-231	1.7	1.0	2.5	5.2
colon	HT-29	2.0	1.2	2.4	5.7
	HCT-15	3.3	2.1	5.8	8.6
lung	A549	1.6	1.0	2.1	6.1
	DMS-114	1.4	1.0	1.2	6.6
prostate	PC-3	0.6	1.4	1.1	3.9
	DU-145	1.3	1.6	1.4	5.6

[a] Tumor cell monolayers were incubated with drug for 72 h. DNA content was measured by CyQuant staining, and IC$_{50}$ values were determined.

Table 3. Data Collection and Refinement Statistics

space group	$P2_12_12_1$
cell dimensions	a = 54.2 Å, b = 72.8 Å, c = 73.5 Å
resolution	2.61 Å
reflections (total)	47878
reflections (unique)	10442
completeness (overall)	99.8%
completeness (last shell)	99.9%
R_{sym} (overall)	4.8%
R_{sym} (last shell)	33.3%
R_{free}	24.2%
R_{conv}	20.1%
mean *B*-factor (overall)	41.2 Å^2
mean *B*-factor (main chain)	44.3 Å^2
rmsd bond lengths	0.007 Å
rmsd bond angles	1.60°

In the complex with H717, CDK2 folds into a two-domain structure with an N-terminal domain that is predominated by β-strands (residues 1−83) and a C-terminal domain which is mostly α-helical (residues 84−298). The ATP-binding site, which is occupied by the inhibitor, is located in a cleft between the two domains (Figure 2). As expected, the overall structure of CDK2 is very similar to the structure of the enzyme in its apo- and ATP-bound[8,21] and other inhibitor-bound forms.[13,20,22] The largest global differences between the ATP and the H717-containing complex structures are observed in the N-terminal domain, whereas the structures of the C-terminal domain are almost identical. The rms positional differences between all Cα atoms is 0.72 Å for an overlay of the complete models, while it is 0.94 Å for an overlay of the N-terminal domain and 0.53 Å for an overlay of the C-terminal domain. The largest local coordinate shift between the two structures is observed at residue Gly147 near the active site.

The N-terminal lobe is involved in extensive crystal contacts. Even minor conformational changes are therefore likely to cause a disruption of packing and hence the observed cracking of the crystals.

Inhibitor Binding in the Active Site. Clear ($F_o - F_c$) difference electron density in the ATP-binding cleft between the two domains indicated unambiguously the location and orientation of the H717 inhibitor molecule. The purine ring system of H717 binds quite differently from the purine portion of the natural cofactor ATP but in a similar way as the homologous but 200-fold weaker inhibitor olomoucine.[20] The ring is embedded between the side chains of Leu134 on one side and Ile10 and

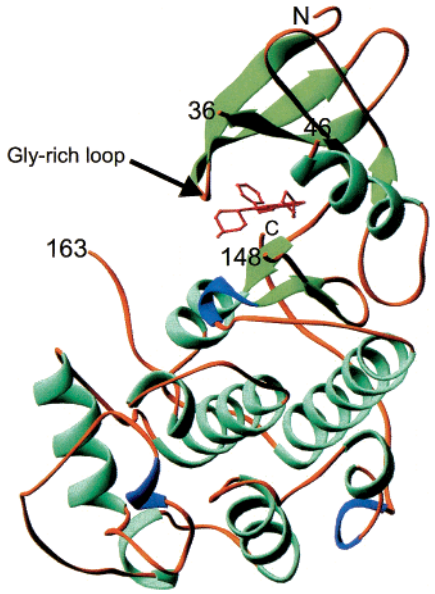

Figure 2. Ribbon representation of the backbone structure of CDK2 showing the location of the inhibitor H717 (red) in the ATP-binding pocket between the (upper) N-terminal and the (lower) C-terminal domains. N- and C-termini as well as residue numbers at chain breaks are indicated.

Ala31 on the other side (Figures 3, 4). An ATP-like orientation for the purine portion of H717 is impossible due to the large benzyl substituent at N-18 which would collide with the backbone around residues Phe80/Glu81, yet the planes of the purine rings deviate only by a few degrees. Similar to other 2,6,9-trisubstituted adenines, H717 forms two strong hydrogen bonds to the Leu83-N and Leu83-O backbone atoms using its N-7 and N-18 atoms as acceptor and donor, respectively. These hydrogen bonds have a more favorable geometry and shorter distance and are therefore assumed to be stronger than the two hydrogen bonds formed between the ATP-purine and this backbone region. Another H-bond is formed between the strongly polarized proton at C-8 of the adenine ring and the main chain carbonyl oxygen of Glu81.

Two large substituents distinguish H717 from the homologous inhibitors roscovitine and olomoucine and account for the different affinities for the enzyme: the cyclopentyl ring at N-9 and the *trans*-diaminocyclohexyl residue at C-2. The cyclopentyl ring binds in a hydrophobic environment formed predominantly by residues Phe80, Val18, and Val64 with smaller contributions from Ala31, Ala144, Leu134, and a more distant polar side made up by main chain and side chain atoms from Asp145. The plane of the cyclopentyl ring is almost perpendicular to the plane of the purine ring and is packed nicely against the aromatic ring of Phe80 with an approximate distance of 4.0 Å between the rings. The two charged amino acid side chains of Asp145 and Lys33 are shifted and rotated away from the hydrophobic ring.

H717 carries a charged amino group at its *trans*-diaminocyclohexane substituent at C-2. The orientation of the cyclohexyl ring differs strikingly from the orientation of the corresponding hydroxyethyl-derived groups in olomoucine, roscovitine, and purvalanol B by a rotation of 180° around the C-2−N-10 bond. This enables the inhibitor to undergo two new interactions with the protein, namely a salt bridge to Asp145-Oδ1 (at 2.7 Å distance) and a hydrogen bond with Asn132-Oδ1 (2.9 Å). Interestingly, the positively charged inhibitor amino group at the 4-position on the cyclohexane is located close to the position of the Mg^{2+} ion in the ATP-binding structure. The shift and rotation of the Asp145 side chain is likely to be responsible for a relatively large conformational change in the main chain of residues 146−148: the backbone at these residues is rather stretched out, while in the other structures it is bent and starts a helical turn in residue Gly147. This results in Cα coordinate shifts of up to 4.4 Å for residues in this stretch of amino acids.

The Cα atoms of Gly11 and Gly13 in the glycine-rich loop between strands β1 and β2 undergo hydrophobic interactions with the C-12 and C-13 atoms in the cyclohexyl ring of H717. Compared to the ATP-containing structure, the loop moves deeper into the cofactor-binding pocket ($\Delta C\alpha = 3.0$ Å for Thr14). A hydrogen bond between Thr14-Oγ and Lys33-Nζ stabilizes this conformation. It should, however, be noted that the glycine-rich loop is still highly mobile.

The aromatic portion of the benzyl substituent at the adenine amino group interacts hydrophobically with the side chains of Ile10 and Phe82 and the main chain of His84 along the edge and on one side of the ring. The other side of the ring is exposed to solvent. The methylene group is involved in van der Waals contact with the main chain at Gln85. An additional methyl group at C-19 as in H724 is sterically unfavorable because it collides with the backbone at Gln85, and hence the inhibition is significantly lower ($IC_{50} = 720$ nM).

Buried Surface Area. Tight and specific binding between a protein and an inhibitor usually requires a high degree of shape complementarity as well as matching of opposite charges and hydrogen bond geometry.[23] One way to describe the geometrical fit is by analysis of the buried solvent-accessible surface areas (SASAs). In an ideal case, the buried SASAs of the two molecules are identical. For the CDK2:H717 complex we determined a total buried SASA of 906 Å^2:521 Å^2 on the inhibitor and 385 Å^2 on the protein. The ratio of 0.74 between buried SASAs of protein and ligand is comparable with data from other complexes.[19] The cyclopentyl ring alone is virtually solvent-inaccessible, and its five atoms contribute 133 Å^2 (26%) to the buried SASA on the inhibitor. The benzyl ring, on the other hand, is relatively accessible for solvent, and its six atoms contribute 82 Å^2 (67%) to the total remaining accessible surface of 123 Å^2 for the bound inhibitor. The shape complementarity as calculated with SC is 0.72 and therefore even higher than for the slightly stronger inhibitor purvalanol B (0.70; calculated from PDB entry 1CKP[8]) and ATP (0.66; calculated from PDB entry 1HCK[13]).

Discussion

The crystal structure of human CDK2 complexed with the adenine-derived inhibitor H717 allows the analysis of inhibitor−enzyme interactions on the atomic level. Particularly interesting are the interactions between the enzyme and the parts of the inhibitor that are different from the related compounds olomoucine, roscovitine, and purvalanol. Although the cyclopentyl ring at N-9 requires more space than the isopropyl group in the

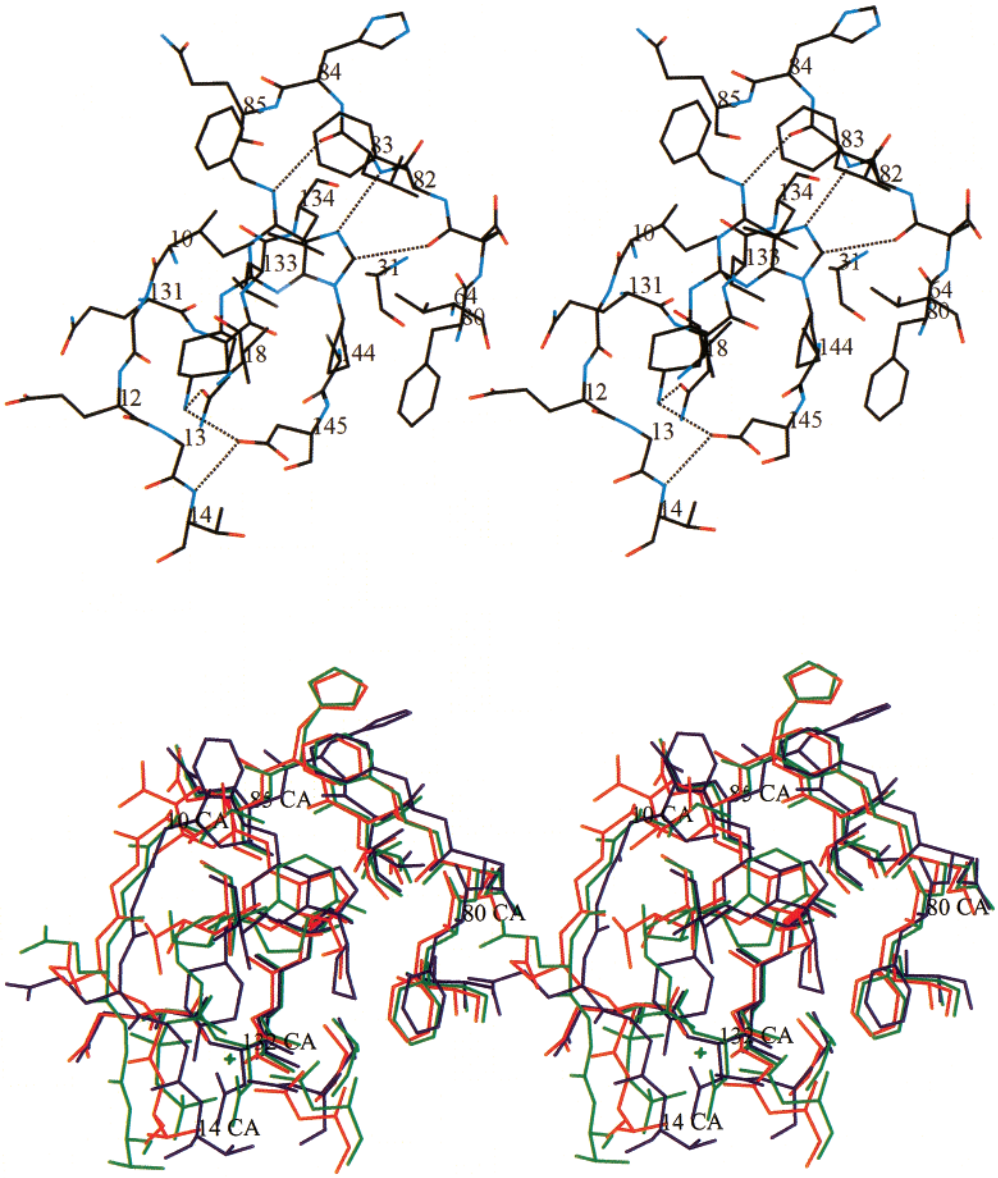

Figure 3. (top) Detailed view of the active site of the CDK2:H717 complex. Polar bonds between the inhibitor and the protein are shown as dotted lines. Oxygen atoms are depicted in red, nitrogen atoms in blue, and carbon atoms in black. Residues are given for the Cα positions. (bottom) Superposition of the active sites of CDK2 in the complexes with H717 (blue), with purvalanol B (red), and with ATP (green). The single green cross indicates the Mg^{2+} ion in the ATP-containing structure.

other inhibitors, it may enhance binding by offering a larger surface area for hydrophobic interactions. In the apo-enzyme as well as in the ATP-containing enzyme, this space next to the adenine ring is empty, and it is only partly occupied by a methyl group and an isopropyl group, respectively, in the olomoucine and roscovitine complexes. Binding of H717 therefore requires only minor rearrangements in the immediate protein environment of the cyclopentyl ring.

To our knowledge, H717 is the first adenine-derived inhibitor that has a positive charge at the C-2 substituent. This *trans*-diaminocyclohexyl group colocalizes with the α-phosphate in a superimposition with the Mg^{2+}/ATP-containing crystal structure.[21] The amino group is close to the position of the Mg^{2+} ion that binds to the phosphates and to Asp145 of CDK2 (Figure 3). The ionic interaction of Asp145 is therefore retained in the complex with H717 and may act as an additionally supportive element for tight binding.

As shown by compound H327, *meta*-halogenation on the phenyl ring does not significantly affect inhibition. This is consistent with the finding that one of the two *meta*-positions is completely exposed to solvent and no interaction with protein atoms is evident to arise from small substituents. The small contribution to binding by the aromatic ring atoms beyond the *ortho*-positions is underscored by the fact that a cyclopropyl ring as in H622 gives an even slightly lower IC_{50} value.

The crystal structure of human CDK2 in complex with H717 broadens the understanding of inhibitor−protein interactions for this important class of enzymes and opens the potential for the structure-based design of additional potent drugs. The antiproliferative properties of the compunds described here suggest that highly active compounds in this chemical series could serve as potential anticancer agents. For instance, some CDK inhibitors, including flavopiridol, are currently in clinical trials for several tumor types.[24]

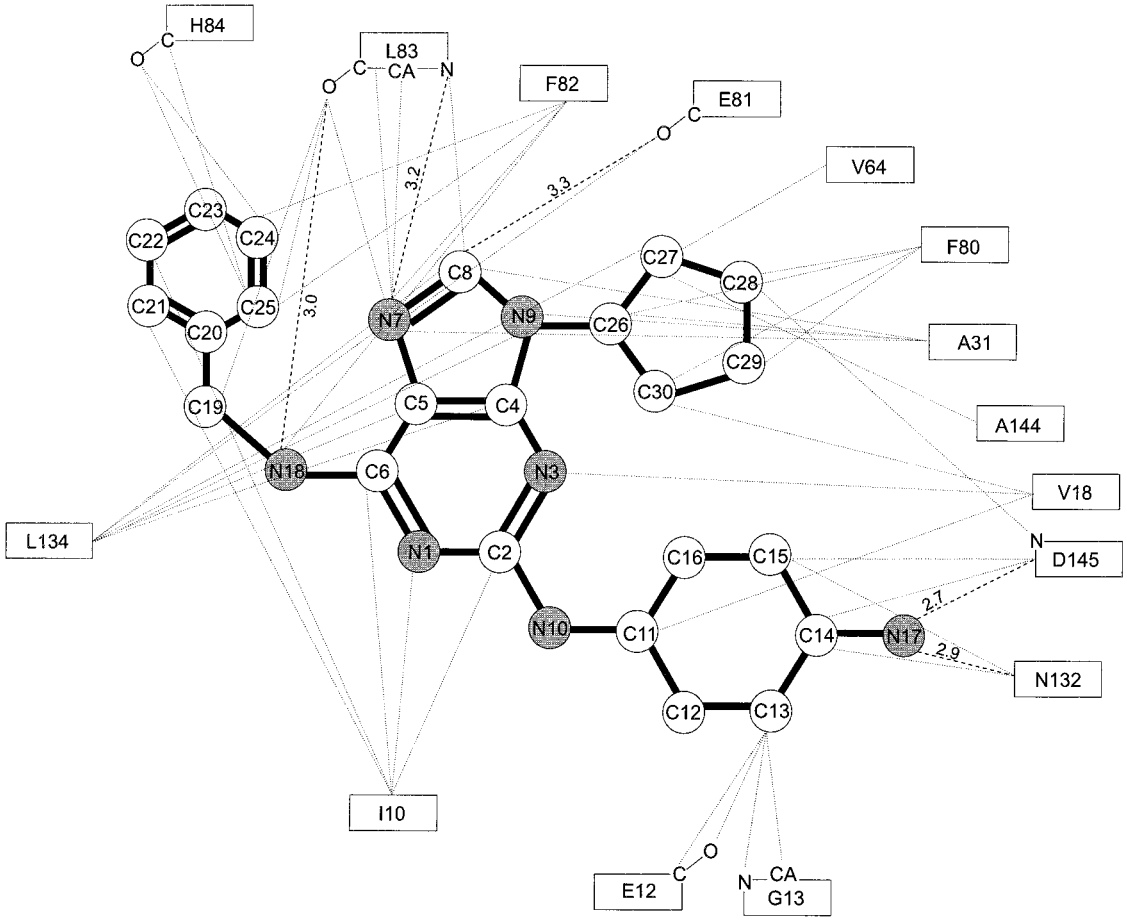

Figure 4. Schematic drawing of interactions between H717 and CDK2. Dotted lines represent nonpolar and broken lines polar bonds with distances given in Å. For clarity, only interactions up to 4.0 Å are shown. Carbon atoms of the inhibitor are shown as white and nitrogen atoms as gray circles. Contacts to CDK2 side chain atoms are indicated by lines to the respective box boundaries while interactions to main chain atoms are shown as lines to the specific atoms.

Experimental Section

Inhibitor Synthesis: Synthesis of 9-Cyclopentyl-2,6-dichloropurine. To a stirred solution of cyclopentanol (2.28 g, 26.5 mmol), 2,6-dichloropurine (5.0 g, 31.8 mmol) and triphenylphosphine (8.33 g, 31.8 mmol) in dry THF (100 mL) at 0 °C was added diethyl azodicarboxylate (5.53 g, 3.60 mmol) dropwise under N_2 atmosphere. The resulting solution was stirred for 48 h at ambient temperature. The reaction mixture was concentrated and the residue was stirred with ether for 2 h. The solid was removed by filtration and the filtrate was concentrated and purified on a 40-g silica gel column which was eluted with methylene chloride to give 4.4 g of product: NMR ($CDCl_3$, TMS) δ 8.13 (s, 1H), 4.95 (quint, 1H), 2.34 (m, 2H), 2.1−1.7 (m, 6H).

Synthesis of 2-[*trans*-(4-Aminocyclohexyl)amino]-6-(benzylamino)-9-cylopentylpurine Dihydrochloride. A solution of 9-cyclopentyl-2,6-dichloropurine (0.5 g, 2.0 mmol), diisopropylethylamine (1 g), and benzylamine (0.21 g, 2.0 mmol) in EtOH (25 mL) was heated at reflux overnight. The solution was concentrated, dissolved in methylene chloride and extracted with water and brine. The aqueous layer was extracted twice with methylene chloride and the combined organic layers were dried over sodium sulfate and concentrated to dryness. The product was transferred to a thick-walled seal tube with 4.0 g of *trans*-1,4-diaminocyclohexane, sealed and heated at 120−140 °C (oil bath), and left overnight. The product was dissolved in methylene chloride and extracted with water and brine. The aqueous layer was extracted three times with methylene chloride and the combined organic phases were dried over sodium sulfate and concentrated to dryness. The product was purified on silica gel using 4:1 methylene chloride/methanol, then converted to the dihydrochloride salt by dissolving the product in ethanol and adjusting the pH to 2.0 with 6 N HCl. The solution was concentrated to give 738 mg of product. Anal. Calcd for $C_{23}H_{31}N_7 \cdot 2.8HCl \cdot 0.5EtOH$: C 54.32, H 6.99, N 18.48. Found: C 54.24, H 7.29, N 18.53.

Substrate for CDK2 and CDK4 Assays. Glutathione-*S*-transferase−retinoblastoma fusion protein (GST-Rb) was obtained from Dr. William Kaelin. GST-Rb was prepared by transformation of *E. coli* with the plasmid pGEX-Rb (379−928) and purified on GSH-Sepharose as described.[25] The transformed bacteria were grown overnight to saturation, then diluted in L broth and incubated at 37 °C for 2 h. The protein was induced by incubation with 0.2 mM isopropyl thioglycoside for 3 h. Following sedimentation by centrifugation, the cells were lysed by sonication in TNEN (50 mM Tris, pH 7.5, 120 mM NaCl, 1 mM EDTA and 0.5% Nonidet P-40). Particulate matter was removed by centrifugation and the lysate was incubated with glutathione-Sepharose at 4 °C. The beads were washed with kinase buffer and then quantitation of Coomassie blue-stained proteins separated by SDS−PAGE was performed using a protein standard of known concentration.

CDK2:Cyclin E Preparation. Recombinant baculoviruses for human CDK2 and cyclin E were obtained from Prof. David Morgan at UC, San Francisco.[26] Optimum coexpression in Sf9 insect cells was obtained at MOI's of 0.1 and 1.0 for CDK2 and cyclin E, respectively, at 72 h post-infection.

Lysates were prepared by lysis of Sf9 cells coinfected with CDK2 and cyclin E in 50 mM HEPES, pH 7.5, 10 mM $MgCl_2$, 1 mM DTT, 0.1 mM phenylmethanesulfonyl fluoride, 5 μg/mL aprotinin, and 5 μg/mL leupeptin using a Parr bomb under 500 psi nitrogen pressure for 5 min at 4 °C. Insoluble material was sedimented at 10000*g* for 20 min at 4 °C. Glycerol was

added to the supernatant to 10% and stored at −80 °C in aliquots.

CDK4:Cyclin D1 Preparation. Human CDK4 was cloned by PCR using degenerate primers based on the published amino acid sequence.[27] The cDNA for human cyclin D1 was cloned by reverse transcription PCR using genomic DNA from MCF-7 cells. The sequence was consistent with the published sequence.[28] Both the cDNAs for CDK4 and cyclin D1 were cloned into pFastBac (Life Technologies), and recombinant Bacmid DNA containing the cDNAs was produced by site-specific transposition using the Bac-to-Bac system (Life Technologies). Bacmid DNA was used to transfect Sf9 insect cells to produce recombinant virus. Following plaque purification of the virus, the viral preparations were amplified until high-titer stocks were achieved. Optimum coexpression of the recombinant proteins was determined to be achieved with an MOI of 0.1 for both CDK4 and cyclin D1 at 72 h post-infection. Insect cell lysates were prepared as described for CDK2:cyclin E.

CDK2:Cyclin E and CDK4:Cyclin D1 Kinase Assay. Millipore Multiscreen 96-well filter plates (0.65-μm Durapore filters, Millipore #MADV NOB50) were prewetted with 200 μL kinase buffer (50 mM Hepes, pH 7.5, 10 mM $MgCl_2$, 1 mM EGTA). GST-Rb (0.5 μg) bound to glutathione-Sepharose beads was added in 50 μL/well and the solution removed by application of vacuum. The assay contained 50 mM Hepes, pH 7.5, 10 mM $MgCl_2$, 1 mM EDTA, 1 mM DTT, 10 mM β-glycerophosphate, 0.1 mM sodium orthovanadate, 0.1mM NaF, 0.25% BSA, 10 μM ATP and 0.25 μCi of [γ^{33}P]ATP (NEN #NEG-602H, 1000−3000 Ci/mmol). Enzyme, 0.1 ng CDK/cyclin (from clarified insect cell lysate), was added to initiate the assay and incubation was for 30 min at 30 °C. Final assay volume was 100 μL. The reaction was terminated by filtration on Millipore vacuum manifold followed by washing four times with TNEN. After drying the plates at room temperature, the filter plates were placed in adapter plates (Packard) and 40 μL of Microscint-O was added to each well. Top Seal A film was used to cover the plates before counting in a Top Count scintillation counter.

CDK1/Cyclin B Preparation. Human CDK1 was cloned by reverse transcription PCR. The sequence was consistent with that reported by Lee and Nurse.[29] The cDNA for cyclin B1 was also cloned by reverse transcription PCR and the sequence was consistent with that reported by Pines and Hunter.[30] CDK1 and cyclin B1 were coexpressed in Sf9 insect cells where optimum coexpression was achieved at an MOI of 0.1 for both CDK1 and cyclin B1 at 48 h post-infection.

CDK1/Cyclin B Kinase Assay. The p34cdc2 SPA [γ^{33}-P] kinase enzyme assay kit was purchased from Amersham Life Science (catalog #RPNQ0170) and the protocol was performed as a 96-well format assay as suggested by the manufacturer. Each assay contained 50 mM Tris HCl, pH 8.0, 10 mM $MgCl_2$, 0.1 mM Na_3VO_4, 0.5 μM ATP, 0.2 μCi [γ-^{33}P]ATP, 2 μM DTT and 0.75 μM biotinylated peptide (biotin-PKTPKKAKKL, derived from the in vitro p34cdc2 phosphorylation site of histone H1) and 3 μg CDK1/cyclin B insect cell lysate in a total assay volume of 100 μL. Incubation was for 30 min at 30 °C. The reaction was terminated by addition of 200 μL of stop buffer (50 μM ATP, 5 mM EDTA, 0.1%(v/v) Triton X-100 in phosphate-buffered saline)/streptavidin-coated SPA beads (2.5 mg/mL). The plate was left at room temperature overnight, covered with a Packard TopSeal and counted on a Packard TopCount.

Antiproliferative Assay. The CyQUANT cell proliferation assay was used to quantitate tumor cell proliferation. Tumor cells were harvested with trypsin−EDTA, and cells that excluded trypan blue were counted, added to 96-well plates and incubated overnight at 37 °C. Drug was added to the wells following dilution in culture medium. Three days later the medium was removed and the plates were frozen at −80 °C for at least 30 min. After the plates had thawed, 200 μL of CyQUANT-GR in cell lysis buffer (Molcular Probes #C-7026) was added to each well and incubated 3−5 min at room temperature. Fluorescence of CyQUANT-GR was measured on a Molecular Devices Fmax fluorescence microplate reader (excitation 485 nm, emission 530 nm).

"Protected" Crystal Cross-Linking. Human CDK2 was purified and crystallized as described elsewhere.[31] Crystals of CDK2 dissolved quickly when H717 was added to the sitting drop, and cocrystallization with the inhibitor was not successful. We therefore cross-linked the crystals as follows: crystals were transferred from the drop to a solution of 0.5 mM ATP, 1 mM $MgCl_2$, 50 mM Hepes (pH 7.4) in order to occupy the active site with the cofactor and hence protect active site lysine residues from potential reaction with the cross-linking agent. The solution was exchanged for 0.1% glutaraldehyde, 50 mM Hepes (pH 7.4) and this cross-linking reaction was kept at 4 °C for 2 h. Subsequently, the crystals were extensively washed with 0.4 M Hepes (pH 7.4) before a few grains of H717 were added to the drop. After 16 h the protein crystals were slightly red in color.

Data Collection and Structure Refinement. X-ray diffraction data of the CDK2:H717 complex were collected with a Rigaku R-AXIS IIC imaging plate on a Rigaku RU-200B rotating anode at 7 °C. Data were processed with DENZO and SCALEPACK.[32] Initial phases were obtained from the protein part of the Mg^{2+}:ATP-containing structure of CDK2,[20] leaving out the flexible regions 36−48 and 147−162. After rigid body and group *B*-factor refinement with X-PLOR[33] the ($F_o - F_c$) difference electron density showed clearly the presence of the inhibitor. Further steps involved manual model building with program "O"[34] and torsion angle molecular dynamics simulated annealing procedures with CNS,[35] using the maximum likelihood target function and bulk solvent correction. All reflections to 2.61 Å resolution were used. The polypeptide chain was refined to convergence before the inhibitor molecule was fitted into the active site pocket, and final steps included alternating cycles of manual rebuilding and maximum likelihood energy minimization. Water molecules were introduced at positions with difference electron density of at least 3.5σ and reasonable hydrogen bond geometry. Because individual *B*-factor refinement did not lead to a significant drop in R_{free}, only grouped *B*-factors (side chain atoms, main chain atoms, and water molecules) were determined. In a later stage, individual *B*-factors were refined for the inhibitor atoms. Structural analysis and calculation of the SASAs (probe radius 1.4 Å) were carried out with X-PLOR, calculation of shape complementarity with SC,[36] and PROCHECK[36] was used for validation of the structure. Figures were produced with Ribbons[37] and O/OPLOT.[34]

Coordinates. Atomic coordinates have been deposited in the Protein Data Bank under accession code 1G5S.

Acknowledgment. Part of this work was supported by a Feodor-Lynen Fellowship from the Alexander-von-Humboldt Gesellschaft (to M.K.D.). This work was also supported by the Director, Office of Science, Office of Biological and Environmental Research, of the U.S. Department of Energy under Contract No. DE-AC03-76SF00098. We are grateful to Andy Thunnissen for discussions and Jaru Jancarik for help with crystallization.

References

(1) Morgan, D. O. Cyclin-dependent kinases: engines, clocks, and microprocessors. *Annu. Rev. Cell. Dev. Biol.* **1997**, *13*, 261−291.
(2) Fesquet, P.; Labbe, J.-L.; Derancourt, J.; Capony, J.-P.; Galas, S.; Girard, F.; Laorca, T.; Shuttleworth, J.; Doree, M.; Cavadore, J.-C. The MO15 gene encodes the catalytic subunit of a protein kinase that activates cdc2 and other cyclin-dependent kinases (CDKs) through phosphorylation of Thr161 and its homologues. *EMBO J.* **1993**, *12*, 3111−3121.
(3) Poon, RY.; Yamashita, K.; Adamczewski, JP.; Hunt, T.; Shuttleworth, J. The cdc2-related protein p40MO15 is the catalytic subunit of a protein kinase that can activate p33cdk2 and p34cdc2. *EMBO J.* **1993**, *12*, 3123−3132.
(4) Arellano, M.; Moreno, S. Regulation of CDK/cyclin complexes during the cell cycle. *Int. J. Biochem. Cell Biol.* **1997**, *29*, 559−573.

(5) Weinberg, R. A. The retinoblastoma protein and cell cycle control. *Cell* **1995**, *81*, 323−330.
(6) Kitagawa, M.; Higashi, H.; Suzuki-Takahashi, I.; Segawa, K.; Hanks, S. K.; Taya, Y.; Nishimura, S.; Okuyama, A. Phosphorylation of E2F-1 by cyclin A-cdk2. *Oncogene* **1995**, *10*, 229−236.
(7) Ziebold, U.; Bartsch, O.; Marais, R.; Ferrari, S.; Klempnauer, K. H. Phosphorylation and activation of B-Myb by cyclin A-Cdk2. *Curr. Biol.* **1997**, *7*, 253−260.
(8) De Bondt, H. L.; Rosenblatt, J.; Jancarik, J.; Jones, H. D.; Morgan, D. O.; Kim, S. H. Crystal structure of cyclin-dependent kinase 2. *Nature* **1993**, *363*, 595−602.
(9) Jeffrey, P. D.; Russo, A. A.; Polyak, K.; Gibbs, E.; Hurwitz, J.; Massague, J.; Pavletich, N. P. Mechanism of CDK activation revealed by the structure of a cyclinA-CDK2 complex. *Nature* **1995**, *376*, 313−320.
(10) Brown, N. R.; Noble, M. E.; Endicott, J. A.; Johnson, L. N. The structural basis for specificity of substrate and recruitment peptides for cyclin-dependent kinases. *Nat. Cell Biol.* **1999**, *1*, 438−443.
(11) Harper, J. W.; Elledge, S. J. Cdk inhibitors in development and cancer. *Curr. Opin. Genet. Dev.* **1996**, *6*, 56−64.
(12) Kamb, A.; Gruis, N. A.; Weaver-Feldhaus, J.; Liu, Q.; Harshman, K.; Tavtigian, S. V.; Stockert, E.; Day, R. S.; Johnson, B. E.; Scolnick, M. H. A cell cycle regulator potentially involved in genesis of many tumor types. *Science* **1994**, *264*, 436−440.
(13) Gray, N. S.; Wodicka, L.; Thunnissen, A. M.; Norman, T. C.; Kwon, S.; Espinoza, F. H.; Morgan, D. O.; Barnes, G.; LeClerc, S.; Meijer, L.; Kim, S. H.; Lockhart, D. J.; Schultz, P. G. Exploiting chemical libraries, structure, and genomics in the search for kinase inhibitors. *Science* **1998**, *281*, 533−538.
(14) Kim, S. H.; Schulze-Gahmen, U.; Brandsen, J.; de Azevedo, W. F., Jr. Structural basis for chemical inhibition of CDK2. *Prog. Cell Cycle Res.* **1996**, *2*, 137−145.
(15) Meijer, L.; Kim, S. H. Chemical inhibitors of cyclin-dependent kinases. *Methods Enzymol.* **1997**, *283*, 113−128.
(16) David-Pfeuty, T. Potent inhibitors of cyclin-dependent kinase 2 induce nuclear accumulation of wild-type p53 and nucleolar fragmentation in human untransformed and tumor-derived cells. *Oncogene* **1999**, *18*, 7409−7422.
(17) Sielecki, T. M.; Boylan, J. F.; Benfield, P. A.; Trainor, G. L. Cyclin-dependent kinase inhibitors: Useful targets in cell cycle regulation. *J. Med. Chem.* **2000**, *43*, 1−18.
(18) Gray, N., Detivaud, L.; Doerig, C.; Meijer, L. ATP-site directed inhibitors of cyclin-dependent kinases. *Curr. Med. Chem.* **1999**, *6*, 859−875.
(19) De Azevedo, W. F.; Leclerc, S.; Meijer, L.; Havlicek, L.; Strnad, M.; Kim, S. H. Inhibition of cyclin-dependent kinases by purine analogues: crystal structure of human cdk2 complexed with roscovitine. *Eur. J. Biochem.* **1997**, *243*, 518−526.
(20) Schulze-Gahmen, U.; Brandsen, J.; Jones, H. D.; Morgan, D. O.; Meijer, L.; Vesely, J.; Kim, S. H. Multiple modes of ligand recognition: crystal structures of cyclin-dependent protein kinase 2 in complex with ATP and two inhibitors, olomoucine and isopentenyladenine. *Proteins* **1995**, *22*, 378−391.
(21) Schulze-Gahmen, U.; De Bondt, H. L.; Kim, S.-H. High-resolution crystal structures of human cyclin-dependent kinase 2 with and without ATP: bound waters and natural ligand as guides for inhibitor design. *J. Med. Chem.* **1996**, *39*, 4540−4546.
(22) De Azevedo, W. F., Jr.; Mueller-Dieckmann, H. J.; Schulze-Gahmen, U., Worland, P. J.; Sausville, E.; Kim, S. H. Structural basis for specificity and potency of a flavonoid inhibitor of human CDK2, a cell cycle kinase. *Proc. Natl. Acad. Sci. U.S.A.* **1996**, *93*, 2735−2740.
(23) Conte, L. L.; Chothia, C.; Janin, J. The atomic structure of protein−protein recognition sites. *J. Mol. Biol.* **1999**, *285*, 2177−2198.
(24) Senderowicz, A. M.; Sausville, E. A. Preclinical and clinical development of cyclin-dependent kinase modulators. *J. Natl. Cancer Inst.* **2000**, *92*, 376−387.
(25) Kaelin, W. G., Jr.; Pallas, D. C.; DeCaprio, J. A.; Kaye, F. J.; Livingston, D. M. Identification of cellular proteins that can interact specifically with the T/E1A-binding region of the retinoblastoma gene product. *Cell* **1991**, *64*, 521−532.
(26) Desai, D.; Gu, Y.; Morgan, D. O. Activation of human cyclin-dependent kinases in vitro. *Mol. Biol. Cell* **1992**, *3*, 571−582.
(27) Matsushime, H.; Ewen, M. E.; Strom, D. K.; Kato, J.-Y.; Hanks, S. K.; Roussel, M. F.; Sherr, C. Identification and properties of an atypical catalytic subunit (p34PSK-J3/cdk4) for mammalian D type G1 cyclins. *Cell* **1992**, *71*, 323−334.
(28) Xiong, Y.; Connolly, T.; Futcher, B.; Beach, D. Human D-type cyclin. *Cell* **1991**, *65*, 691−699.
(29) Lee, M. G.; Nurse, P. Complementation used to clone a human homologue of the fission yeast cell cycle control gene cdc2. *Nature* **1987**, *327*, 31−35.
(30) Pines, J.; Hunter, T. Isolation of a human cyclin cDNA: evidence for cyclin mRNA and protein regulation in the cell cycle and for interaction with p34cdc2. *Cell* **1989**, *58*, 833−846.
(31) Rosenblatt, J.; De Bondt, H.; Jancarik, J.; Morgan, D. O.; Kim, S. H. Purification and crystallization of human cyclin-dependent kinase 2. *J. Mol. Biol.* **1993**, *230*, 1317−1319.
(32) Otwinowski, Z.; Minor, W. Processing of X-ray diffraction data collected in oscillation mode. *Methods Enzymol.* **1997**, *276 A*, 307−326.
(33) Brunger, A. T. *X-PLOR, a system for X-ray crystallography and NMR*; Yale University: New Haven, CT, 1992.
(34) Jones, T. A.; Zou, J. Y.; Cowan, S. W.; Kjeldgaard, M. Improved methods for building protein models in electron density maps and the location of errors in these models. *Acta Crystallogr. A* **1991**, *47*, 110−119.
(35) Brunger, A. T.; Adams, P. D.; Clore, G. M.; Delano, W. L.; Gros, P.; Grosse-Kunstleve, R. W.; Jiang, J.-S.; Kuszewski, J.; Nilges, M.; Pannu, N. S.; Read, R. J.; Rice, L. M.; Simonson, T.; Warren, G. L. Crystallography & NMR system: A new software for macromolecular structure determination. *Acta Crystallogr. D* **1998**, *54*, 905−921.
(36) Collaborative Computational Project Number 4. The CCP4 Suite: Programs for Protein Crystallography. *Acta Crystallogr. D* **1994**, *50*, 760−763.
(37) Carson, M. Ribbons 2.0. *J. Appl. Crystallogr.* **1991**, *24*, 958−961.

JM001043T